International Journal of Advanced Engineering Research and Science (IJAERS)
Peer-Reviewed Journal
ISSN: 2349-6495(P) | 2456-1908(O)
Vol-13, Issue-4; Apr, 2026
Journal Home Page Available: https://ijaers.com/
Article DOI: https://dx.doi.org/10.22161/ijaers.134.3

Multi-Objective Coordinated Scheduling of Virtual Power Plants for Economic, Low-Carbon, and Stability Objectives: A DOA-NSGAII Hybrid Optimization Strategy

Yu-Xuan Chen*, Yan-Zuo Chang, Yan-Xiao Jia, Kai-Ming Chen, Zi-Rui He, Wen-Min Wen, Guan-Hong Xie, Hong-Rui Yang, Jie-Zhen Yang, Yong-Qing Wang, Zheng-Kuan Deng

School of Energy and Power Engineering, Guangdong University of Petrochemical Technology, Maoming, Guangdong 525000, China
*Corresponding author : 2127951048@qq.com

Received: 24 Feb 2026,
Received in revised form: 27 Mar 2026,
Accepted: 30 Mar 2026,
Available online: 05 Apr 2026

***Keywords*— Mechanical Structural Fatigue, Rainflow Virtual Power Plant, Dream Optimization Algorithm, Multi-Objective Optimization, NSGA-II.**

***Abstract*—** *To achieve low-carbon, economical, and secure operation of power systems under the "dual carbon" goals, virtual power plants (VPPs) serve as a key technology for aggregating flexible resources such as distributed energy, storage, and demand response, making multi-objective coordinated scheduling critically important. However, the high dimensionality, multiple constraints, and conflicting objectives of this problem pose challenges for traditional optimization methods. Therefore, this paper proposes a hybrid intelligent optimization framework based on an improved Dream Optimization Algorithm (DOA) and the Non-dominated Sorting Genetic Algorithm (NSGA-II), termed DOA-NSGAII, to solve the multi-energy scheduling problem of VPPs with objectives of minimizing economic cost, carbon emissions, and peak-valley load difference. Through customized encoding, decoding, and constraint-handling mechanisms, the framework integrates DOA's global search capability with NSGA-II's multi-objective decision-making advantages. Simulation experiments on the IEEE 14-bus system with three comparative schemes show that, compared with the single-objective economic optimization scheme (S1), the proposed multi-objective coordinated optimization scheme (S3) achieves significant comprehensive benefits—reducing carbon emissions by 30.5% and improving the peak-valley load difference by 12.0%—at the cost of only a marginal 4.9% increase in economic cost. This study validates the effectiveness of the DOA-NSGAII framework in solving complex engineering optimization problems and provides a new approach for multi-objective intelligent scheduling of VPPs.*

I. INTRODUCTION

To address global environmental challenges, the global energy transition has driven the large-scale deployment of distributed energy resources (DERs). However, the instability and seasonality exhibited by DERs have hindered the pace of development **Error! Reference source not found.**. Virtual power plants (VPPs), by leveraging adjustable loads and aggregating DERs, have become a key technology for promoting DER applications and enhancing the flexibility of power systems **Error! Reference source not found.**. The grid integration planning and hosting capacity calculation of DERs have also become important prerequisites for resource aggregation in VPPs **Error! Reference source not found.**[4], as a reasonable hosting capacity assessment can effectively improve DER integration efficiency and grid operational stability **Error! Reference source not found.**[6][7].

In a VPP, it is necessary to obtain an optimal solution that meets expectations under the mutual constraints among DERs, energy storage systems, demand response, and grid interaction **Error! Reference source not found.**. To solve such optimization problems, corresponding strategies must be adopted, which serve as the key technology for addressing these issues. Compared with traditional optimization algorithms, metaheuristic algorithms do not require rigorous mathematical proof **Error! Reference source not found.**; instead, they guide the search process using heuristic information, thereby avoiding entrapment in local optima and effectively solving complex real-world problems. Consequently, they have been extensively studied and applied across various fields. The continuous emergence of novel metaheuristic algorithms also provides additional solution ideas for VPP scheduling optimization.

Metaheuristic algorithms are a class of high-level strategic frameworks for solving complex optimization problems. While they do not guarantee finding the global optimum, they can provide high-quality approximate solutions within a reasonable time. Their core concept is to mimic intelligent behaviors observed in natural or social phenomena, guiding the search process through a balance between exploration and exploitation. Among them, the Dream Optimization Algorithm (DOA) is distinguished by its strong global search capability, ability to escape local optima, dynamic balance between exploration and exploitation, and inherent diversity maintenance mechanism. It transforms the creative thinking process of human dreams into an efficient optimization search mechanism, and its core memory-forgetting-sharing framework offers new insights for solving complex optimization problems characterized by high dimensionality, nonlinearity, and multiple peaks **Error! Reference source not found.**. When addressing complex engineering optimization problems such as those encountered in VPPs—which are characterized by high dimensionality, multiple constraints, multiple objectives, and nonlinearity—DOA demonstrates potential advantages over some traditional optimization algorithms in terms of global search capability, solution set diversity, and convergence robustness.

II. VIRTUAL POWER PLANT SYSTEM MODEL

2.1 Virtual Power Plant

As a key technical form for enabling efficient utilization of distributed resources and source-grid-load-storage coordination in new-type power systems, virtual power plants (VPPs) integrate adjustable resources such as distributed energy resources, energy storage, and controllable loads within a region through advanced information communication and intelligent scheduling technologies, thereby forming a dispatchable virtual controllable unit. Centered on digital platforms and driven by market mechanisms, VPPs aggregate dispersed resources into an integrated entity with regulation capabilities equivalent to those of traditional power plants. They can participate in auxiliary services such as peak shaving and frequency regulation, as well as electricity trading, thereby enhancing renewable energy integration capability, smoothing power fluctuations, and reducing system operating costs. As such, VPPs represent an important technology for supporting the achievement of carbon peak and carbon neutrality goals. Because electricity production, transmission, and consumption occur simultaneously and cannot be stored on a large scale, the power output from distributed sources and the grid interaction power must remain balanced with the load demand at any given time within the VPP. This balance is expressed by the following constraint:

$$\mathrm{P_{WT}(t) + P_{PV}(t) + P_{GT}(t) + P_{grid}(t) + P_{BESS}(t) = L_{base}(t) + \Delta L(t)} \quad (1)$$

where $P_{WT}(t)$ is the wind power output, $P_{PV}(t)$ is the photovoltaic power output, $P_{GT}(t)$ is the gas turbine output, $P_{grid}(t)$ is the grid interaction power, $P_{BESS}(t)$ is the energy storage system power, $L_{base}(t)$ is the base load, and $\Delta L(t)$ is the load variation, i.e., the demand response amount.

If the power system fails to maintain real-time generation–consumption balance, a situation may arise where the sum of distributed generation output and grid interaction power exceeds the load demand. In this case, the surplus electrical energy, having nowhere to be absorbed, is converted into kinetic energy in the generator rotors,

causing the system frequency to increase. Conversely, when the sum of distributed generation output and grid interaction power falls short of the load demand, the resulting energy deficit slows down the generator rotors, leading to a decrease in system frequency.

2.2 Distributed Energy Resource Model

Distributed energy resources (DERs) are small-scale, decentralized energy systems developed near the consumer side. They are characterized by flexible siting, local consumption, and clean, low-carbon operation, complementing centralized energy systems and serving as an important component of new-type power systems. However, due to their small individual capacities, the intermittency of wind power constrained by wind speed variability, and the dependence of photovoltaics on solar irradiance and weather conditions, DERs exhibit nonlinear and seasonal characteristics. As a result, they need to be aggregated and managed through virtual power plants (VPPs). The DERs involved include wind power, photovoltaics, and gas turbines. Among them, gas turbines ensure supply stability at the cost of high operational expenses and carbon emissions, necessitating coordinated optimization strategies to balance the operation of the three resources to achieve economic and carbon reduction objectives. Owing to the uncontrollability, volatility, and forecasting uncertainty of wind and solar power caused by natural conditions, the actual output of wind turbines and photovoltaic systems must not exceed the predicted maximum values. This constraint is expressed as follows

$$0 \le P_{WT}(t) \le P_{WT,max}(t), 0 \le P_{PV}(t) \le P_{PV,max}(t) \quad (2)$$

where $P_{WT,max}(t)$ and $P_{PV,max}(t)$ represent the predicted maximum output of wind power and photovoltaics during period t, respectively.

2.2.1 Wind Power Generation Model INDENTATIONS AND EQUATIONS.

The output power of a wind turbine is strongly correlated with the real-time wind speed. A wind speed–power characteristic model commonly used in engineering applications is adopted:

$$P_{WT} = \begin{cases} 0, & v(t) < v_{ci} \text{或 } v(t) > v_{co} \\ P_{WT,r} \times \dfrac{v(t)^3 - v_{ci}^3}{v_r^3 - v_{ci}^3}, & v_{ci} < v(t) \le v_r \\ P_{WT,r}, & v_r \le v(t) \le v_{co} \end{cases} \quad (3)$$

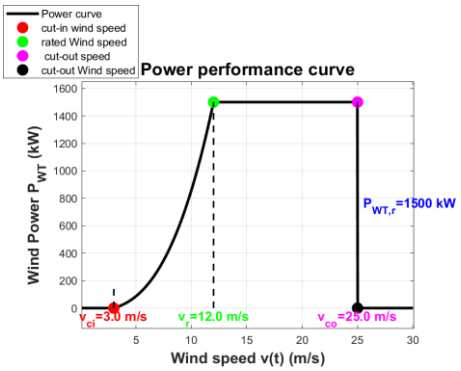

Fig. 1. Power characteristic curve of the wind turbine.

where $v(t)$ is the real-time wind speed at the hub height during period t, in m/s; v_{ci}, v_{co}, and v_r denote the cut-in wind speed, cut-out wind speed, and rated wind speed of the wind turbine, respectively. According to the figure, the values adopted in this paper are v_{ci} = 3 m/s, v_{co} = 25 m/s, and v_r = 12 m/s;$P_{WT,r}$ represents the rated power of the wind turbine, in kW. This model is suitable for system-level simulation and capacity planning, and the resulting data can be used for accurate short-term forecasting or performance evaluation.

2.2.2 Photovoltaic Power Generation Model

The output power of a photovoltaic (PV) cell is related to solar irradiance and ambient temperature. To predict the electrical power output of PV generation, the following model is constructed:

$$P_{PV}(t) = P_{Pv,r} \times \frac{G(t)}{G_{STC}} \times [1 + \alpha_T \cdot (T(t) - T_{STC})] \quad (4)$$

where $P_{PV,\ r}$ is the rated power of the PV module, in kW; G(t) is the real-time solar irradiance during period \(t\), in W/m²; GSTC is the solar irradiance under standard test conditions, taken as 1000 W/m²; α_T is the power temperature coefficient, taken as –0.43%; T(t) is the panel temperature during period t, in °C; and T_{STC} is the standard test temperature, taken as 25°C.

2.2.3 Gas Turbine Model

As a controllable and adjustable power source, the gas turbine serves to compensate for power deficits and provide peak shaving . Its output power is subject to the following constraint:

$$0 \le P_{GT}(t) \le P_{GT,max} \quad (5)$$

where $P_{GT,max}$ is the rated output of the gas turbine, taken as 800 kW in this paper.

The output variation of the gas turbine between adjacent periods is limited by the ramping rate, and this constraint is expressed as follows:

$$-\mathrm{R_{down}} \le \mathrm{P_{GT}(t)} - \mathrm{P_{GT}(t-1)} \le \mathrm{R_{up}} \quad (6)$$

where R_{down} and R_{up} are the maximum downward and upward ramping rates of the gas turbine, respectively, both taken as 200 kW/h in this paper.

2.3 Energy Storage System Model

Energy storage systems serve as core equipment for achieving spatiotemporal transfer of energy and enhancing the regulation capability of power systems, offering advantages such as fast response, high precision, and bidirectional power controllability. They can smooth fluctuations in renewable energy generation, perform peak shaving and valley filling, and improve power supply reliability. In virtual power plants (VPPs), energy storage acts as a key adjustable resource, undertaking the functions of energy buffering and power support, thereby providing flexible regulation capabilities for the VPP and serving as an important foundation for source-grid-load-storage coordination. To improve resource utilization efficiency, a lithium-ion battery energy storage model is adopted in this paper. Its core is the time-sequential recursive relationship of the state of charge (SOC), which describes the dynamic process of energy storage, expressed as follows:

$$\mathrm{SOC(t)} = \big(\mathrm{SOC(t-1)}\big) + \frac{\eta_c \cdot \max(-\mathrm{P_{BESS}(t)}.0) - \frac{\max\big((\mathrm{P_{BESS}(t)}.0)\big)}{\eta_d}}{\mathrm{E_{BESS}}} \cdot \Delta t \quad (7)$$

where SOC(t) and SOC(t-1) represent the state of charge (SOC) of the energy storage system at the end of periods t and t-1, respectively; η_c and η_d are the charging and discharging efficiencies of the energy storage system, respectively, both taken as 0.95 in this paper; E_{BESS} is the rated capacity of the energy storage system, taken as 1000 kW·h in this paper; and Δt is the time step, set to 1 h.

The operation of the energy storage system is subject to the following constraints:

$$\begin{cases} \mathrm{P_{BESS,ch,max}} \le \mathrm{P_{BESS}(t)} \le \mathrm{P_{BESS,dch,max}} \\ \mathrm{SOC_{min}} \le \mathrm{SOC(t)} \le \mathrm{SOC_{max}} \\ \mathrm{SOC(0)} = \mathrm{SOC(24)} \end{cases} \quad (8)$$

where $P_{BESS,ch,max}$ and $P_{BESS,dch,max}$ are the maximum charging and discharging power of the energy storage system, respectively, taken as −300 kW and 300 kW in this paper; SOC_{min} and SOC_{max} are the lower and upper limits of the SOC, taken as 0.2 and 0.8, respectively; and SOC(0) = SOC(24) is the equality constraint ensuring that the SOC at the beginning and end of the scheduling period are equal, thereby guaranteeing the integrity of the scheduling cycle.

2.4 Demand Response Model

Demand response (DR) is an interactive mechanism through which users actively adjust their electricity consumption in response to grid conditions, prices, or incentive signals. It can transform passive consumers into flexible regulation resources by reducing or shifting loads during peak periods or grid fluctuations, thereby alleviating grid stress, facilitating renewable energy integration, and generating benefits for users. Within the virtual power plant (VPP) framework, DR is deeply integrated with distributed energy resources (DERs) and energy storage systems, and through aggregation and coordinated control, it forms a scalable adjustable capability that serves as an important pillar for VPP participation in grid interaction and electricity market transactions. Incorporating DR into multi-energy coordinated scheduling can further enhance the economic and operational performance of VPPs. In this paper, a price-based demand response model is adopted, and the load shifting characteristics in response to electricity price variations are described using a consumer electricity consumption elasticity matrix. The model is expressed as follows:

$$\frac{\Delta \mathrm{L(t)}}{\mathrm{L_{base}(t)}} = \sum_{\tau=1}^{24} \varepsilon_{t,\tau} \cdot \frac{\lambda_{\mathrm{grid}}(\tau) - \lambda_0}{\lambda_0} \quad (9)$$

where ϵ_t, τ is the price elasticity coefficient; when $\tau = t$, it represents the self-elasticity coefficient, and when $\tau = t$ it represents the cross-elasticity coefficient; λ_0 is the base electricity price, in RMB/kWh.

The load variation on the user side is limited by the maximum adjustable capacity, and this constraint is expressed as follows:

$$\Delta \mathrm{L_{min}} \le \Delta \mathrm{L(t)} \le \Delta \mathrm{L_{max}} \quad (10)$$

where $\Delta L_{\min}$ and $\Delta L_{\max}$ are the maximum load reduction and increase amounts, respectively, taken as ±200 kW in this paper.

2.5 Grid Interaction Model

Grid interaction refers to the comprehensive process of information exchange, power exchange, and dispatch coordination between power entities and the grid. It is central to ensuring system stability and enabling bidirectional energy and information flow. With the large-scale integration of consumer-side resources, the complexity of grid interaction has increased, and efficient interaction supports power balance, renewable energy integration, and ancillary services. Within the virtual power plant (VPP) framework, grid interaction serves as the link connecting distributed resources with system dispatch. By employing standardized technologies, the VPP integrates dispersed resources into a unified regulated entity, achieving standardized interaction with the grid, addressing the fluctuations and dispatch challenges associated with distributed resource grid integration, supporting the VPP's participation in various grid services, and promoting the

development of new-type power systems toward intelligence and efficiency. The power interaction between the VPP and the main grid is limited by the tie-line transmission capacity, and this constraint is expressed as follows:

$$P_{grid,min} \le P_{grid}(t) \le P_{grid,max} \quad (11)$$

where $P_{grid,min}$ and $P_{grid,max}$ are the maximum selling and purchasing power of the tie-line, respectively, taken as $P_{grid,min} = -500$ kW and $P_{grid,max} = 800$ kW in this paper.

III. DESIGN OF THE IMPROVED DREAM OPTIMIZATION ALGORITHM

3.1 Dream Optimization Algorithm

The Dream Optimization Algorithm (DOA) is a novel intelligent optimization method inspired by the cognitive mechanisms of brain sleep and dreaming. By simulating processes such as wakeful perception, dream reconstruction, memory consolidation, and state switching, it achieves a dynamic balance between global exploration and local exploitation, demonstrating strong global search capability and convergence stability. Applying DOA to the optimal scheduling problem of virtual power plants (VPPs) effectively addresses challenges such as the diversity of distributed energy resources, energy storage systems, controllable loads, and demand response resources within VPPs, along with complex operational constraints and the multi-peak nonlinear nature of the objective functions. Under constraints such as grid interaction rules, power balance, and equipment operational limits, the algorithm performs global optimization and coordinated allocation of the outputs, charging/discharging powers, and adjustable loads of various resources within the VPP, aiming to minimize operating costs, maximize profits, or maximize renewable energy integration. Compared with traditional optimization methods, DOA can rapidly escape local optima in complex high-dimensional scheduling spaces and obtain superior coordinated scheduling strategies, thereby enhancing the economic efficiency and operational performance of VPPs and strengthening their efficient, stable, and flexible interaction with the grid. This provides an efficient and reliable intelligent solution for the optimal operation of VPPs within new-type power systems.

Algorithm 1 Pseudo-code of DOA

Input: Population size(N_{max}), the lower limits of variables(X_l), the upper limits of variables(X_u), size of problem(Dim), the current number of iteration(t), the number of iteration as a demarcation(T_d), the maximum number of iterations(T_{max}), forgetting dimensions of each group and of exploitation($k_1, k_2, k_3, k_4, k_5, k_r$)
Output: the best solution X_{best} and the minimum fitness $Fitness_{best}$

Generate an initial population X of N individuals using Eqs. (2) and (3)
Check the bounds of the solutions
Evaluate the fitness of the solutions
Detect the best solution X_{best} and the minimum fitness $Fitness_{min}$
Define the current iteration $t = 1$
while $t < T_d$ **do**
  Update the best solution X_{best} and the minimum fitness $Fitness_{min}$
  for $q = 1 : 5$ **do**
    Update the best solution X_{best_q} and the minimum fitness $Fitness_{min_q}$
    Update k_q using Eq. (10)
    Update X_i^{t+1} using Eq. (4)
    $(K_1, K_2, \dots, K_{k_q}) = randperm(k_q, N)$
    for $i = ((q-1)/5 \times N) + 1) : (q/5 \times N)$ **do**
      if $rand < u$ **then**
        Update $x_{i,j}$ using Eq. (5)
        Check the bounds of $x_{i,j}$
      else
        Update $x_{i,j}$ using Eq. (6)
      end if
    end for
  end for
  Update the current number of iteration t by $t = t + 1$
end while
while $t > T_d$ and $t < T_{max}$ **do**
  Update k_r using Eq. (11)
  Update X_i^{t+1} using Eq. (7)
  $(K_1, K_2, \dots, K_{k_r}) = randperm(k_r, N)$
  for $i = 1 : N$ **do**
    Update $x_{i,j}$ using Eq. (8)
    Check the bounds of $x_{i,j}$
  end for
  Update the current number of iteration t by $t = t + 1$
end while

Fig. 2. Pseudo-code of the dream optimization algorithm.

3.1.1 Initialization

Let the dimension of the optimization problem be D (corresponding to the total number of scheduling variables in this paper) and the population size be N. The position of the i-th individual in the g-th generation is denoted as $X_i^g = \left(x_{i,1}^g, x_{i,2}^g, \dots, x_{i,D}^g\right)$, and its fitness value is $f\left(X_i^g\right)$. Within the upper and lower bounds of the decision variables, an initial population $\{X_i^0 \mid i = 1,2,\dots,N\}$ is randomly generated, and the fitness of each initial individual is calculated.

3.1.2 Iterative Process of Dream Optimization

Based on individual fitness rankings, the population is equally divided into K groups (typically $K = 5$). Individuals within each group share the "group best position" of that group, denoted as $GBest_k^g$ (for $k = 1, \dots, K$). This constitutes the grouping and memory encoding step.

During the global exploration phase, two strategies are executed in parallel for each individual X_i^g (belonging to group k), and the better outcome is retained. Strategy A: Forgetting–Supplement Strategy – The individual randomly "forgets" a subset of dimensions according to a forgetting rate ρ_f . For each selected dimension j, the new position is explored as follows:

$$x_{I,j}^{candidate1} = GBest_{k,j}^{g} + \alpha \cdot \left(GBest_{k,j}^{g} - x_{I,j}^{g}\right) \cdot \Delta \quad (12)$$

where α is the exploration step coefficient, and Δ is a random number in $[-1,1]$. This strategy enables guided random perturbations around the group best during the search.

Strategy B: Dream Sharing Strategy – The individual also forgets a subset of dimensions. For each selected

dimension j, the new position is taken from the corresponding dimension of another randomly selected individual r in the population:

$$x_{I,j}^{g+1} = x_{I,j}^{explore} + \beta \cdot \left(Best_{global,j}^{g} - x_{I,j}^{explore}\right) \cdot \mathcal{N}(0,\ 1) \quad (13)$$

where β is the exploitation step coefficient (typically $\beta < \alpha$), and $\mathcal{N}(0,1)$ is a random number drawn from the standard normal distribution. This operation applies small-scale Gaussian perturbations around the global optimum to improve convergence accuracy.

3.1.3 Elite Retention and Iteration

Evaluate the fitness of the new population $\{X_i^{g+1}\}$ and update the global best solution $Best_{global}^{g+1}$. Return to the iterative process of the Dream Optimization Algorithm until the termination condition of reaching the maximum number of iterations $G_{\max}$ is satisfied.

3.2 Adaptation and Implementation of the Dream Optimization Algorithm in Virtual Power Plants

To address key adaptation issues such as variable encoding, constraint handling, and multi-objective integration, the Dream Optimization Algorithm (DOA) is applied to the multi-objective optimization problem of virtual power plants (VPPs) in this paper. The decision variables are defined as the power sequences of the controllable resources over the scheduling horizon ($T = 24$ hours). A complete scheduling scheme is encoded as an individual X_i, with a dimensionality of $D = 72$. The specific encoding is as follows:

$$X_i = \begin{bmatrix} P_{GT}(1), \dots, P_{GT}(24), P_{BESS}(1), \dots, \\ P_{BESS}(24), P_{grid}(1), \dots, P_{grid}(24) \end{bmatrix} \quad (14)$$

where $P_{GT}(t)$ represents the output of the gas turbine during period t, which must satisfy its upper and lower limits as well as ramping constraints; $P_{BESS}(t)$ represents the power of the energy storage system during period t, with positive values indicating discharging and negative values indicating charging, and must satisfy its charging/discharging power and SOC constraints; $P_{grid}(t)$ represents the power exchanged with the main grid during period t, with positive values indicating electricity purchase and negative values indicating electricity sale, and must satisfy the tie-line capacity constraints. The wind power output $P_{WT}(t)$ and photovoltaic output $P_{PV}(t)$ are taken as known forecast values, while the demand response load variation $\Delta L(t)$ is determined by the electricity price elasticity model, grid electricity prices, and baseline load. Neither is directly treated as an optimization variable, but both are involved in power balance calculations and objective function evaluation.

In this paper, a hybrid constraint-handling strategy is adopted to ensure efficient search within the feasible region. The power balance equality constraint is enforced as follows. Before evaluating the fitness of each individual, instead of directly using the encoded $P_{grid}(t)$, its value is calculated in real time based on other variables to satisfy the power balance equation:

$$P_{grid}^{calc}(t) = L_{base}(t) + \Delta L(t) - \left(P_{WT}(t) + P_{PV}(t) + P_{GT}(t) + P_{BESS}(t)\right) \quad (15)$$

This calculated value replaces the corresponding $P\_grid\ (t)$ in the individual encoding for subsequent evaluation. This fundamentally ensures that all solutions satisfy the power balance constraint. To ensure a high-quality product, diagrams and lettering MUST be either computer-drafted or drawn using India ink.

For inequality constraints such as equipment output limits, ramping rates, SOC limits, and tie-line capacity constraints, a static penalty function method is adopted. The total constraint violation is converted into a penalty term and added to the objective function. For example, the total penalty term $Penalty(X_i)$ is expressed as:

$$Penalty(X_i) = \lambda \sum_{t=1}^{24} \left[\max\left(0, P_{GT}(t) - P_{GT,max}\right)^2 + \cdots\right] \quad (16)$$

where λ is the penalty factor. Ultimately, the fitness function of the algorithm is formed by adding this penalty term to the original three objective function values, thereby guiding the search toward the feasible region.

In this paper, the framework of the non-dominated sorting genetic algorithm (NSGA-II) is combined with the search mechanism of the Dream Optimization Algorithm (DOA). After each generation of the DOA iteration produces a new population, the parent and offspring populations are merged. All individuals in the merged population are then subjected to non-dominated sorting based on the three objectives—economic cost, carbon emissions, and peak-valley load difference—and are divided into multiple fronts. Subsequently, the crowding distance of individuals within the same non-dominated front is calculated to measure their distribution density in the objective space. During selection, individuals with a higher non-dominated rank are prioritized; for individuals with the same rank, those with a larger crowding distance are preferred to maintain solution diversity. Finally, according to the above rules, a number of individuals equal to the initial population size are selected as the parent population for the next generation of the DOA iteration.

Given the scale (72 dimensions) and complexity of the virtual power plant (VPP) scheduling problem addressed in this paper, the parameters of the DOA algorithm were set

through preliminary experimental tuning as follows: population size $N = 100$, maximum number of iterations $G_{\max} = 300$, number of groups $K = 5$, initial forgetting rate $p_f = 0.5$ linearly decreasing to 0.1 with iterations, exploration coefficient $\alpha = 0.8$, exploitation coefficient $\beta = 0.2$, and penalty factor $\lambda = 1 \times 10^6$. This parameter set is designed to balance global search capability, convergence speed, and solution feasibility. Through the above adaptations, the Dream Optimization Algorithm has been systematically transformed into a customized intelligent optimizer capable of directly and effectively solving the multi-time-scale, multi-constraint, multi-objective coordinated scheduling problem of virtual power plants.

IV. SIMULATION

The simulation period is 24 hours, with a time resolution of $\Delta t = 1$ h. The typical daily output curves of wind power and photovoltaics, along with the base load curve, are shown in Fig. 3. The grid adopts a time-of-use electricity pricing mechanism, and the specific price signals are illustrated in Fig. 4.

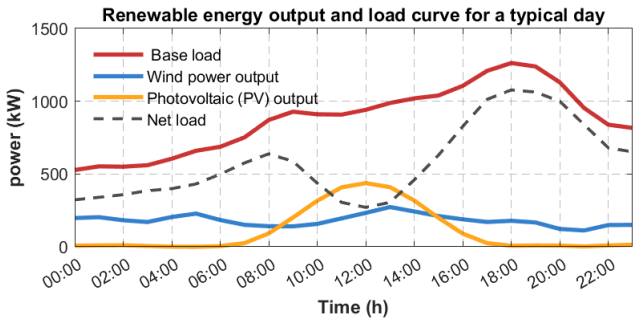

Fig. 3. Typical daily output curves of wind power and photovoltaics, and base load curve.

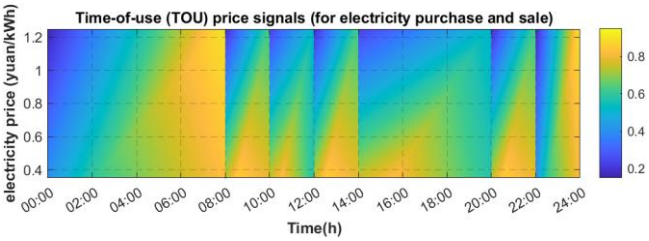

Fig. 4. Time-of-use electricity price signal.

The key parameters of each component within the virtual power plant strictly follow the models established in Chapter 2, and their specific values are summarized in Table 1 to ensure the reproducibility of the model.

Through preliminary experiments of parameter sensitivity analysis, the core parameters of the DOA-NSGAII hybrid algorithm were determined as follows: population size $N = 100$, maximum number of iterations $G_{max} = 300$, number of groups $K = 5$, exploration coefficient $\alpha = 0.8$, exploitation coefficient $\beta = 0.2$, and forgetting rate p_f linearly decreasing from 0.5 to 0.1. The crossover probability and mutation probability in the NSGA-II framework were set to 0.9 and $1/D$ (where $D = 72$ is the dimension of the decision variables), respectively.

4.2 Design of Comparative Schemes

To comprehensively evaluate the effectiveness of the proposed strategy, three comparative schemes were established as follows:

Scheme 1 (S1): Single-objective economic scheduling. The daily operational economic cost is minimized as the sole optimization objective, solved using the standard DOA. The operational strategy of the energy storage system is freely optimized by the algorithm.

Scheme 2 (S2): Fixed-strategy scheduling. The optimization objective is also to minimize economic cost, but the energy storage system adopts a fixed "charge during valley periods, discharge during peak periods" empirical strategy (i.e., charging during low-price periods and discharging during high-price periods), thereby simulating traditional scheduling modes lacking intelligent optimization.

Scheme 3 (S3): Multi-objective coordinated scheduling proposed in this paper. The DOA-NSGAII hybrid algorithm is employed to simultaneously optimize the three objectives of economic cost, carbon emissions, and peak-valley load difference. A comprehensively balanced solution is ultimately selected from the Pareto optimal solution set as the final scheduling scheme.

Table 1. Simulation parameters of the virtual power plant

Component/Parameter	Symbol	Value	Unit
gas turbine	rated power	$P_{GT,max}$	800
	ramping rate	R_{up}, R_{down}	200
lithium-ion battery energy storage	rated capacity	E_{BESS}	1000
	rated power	$P_{BESS,ch,max}/P_{BESS,dch,max}$	±300
	SOC limits	SOC_{min}/SOC_{max}	0.2/0.8
	charging/discharging efficiency	η_c/η_d	0.95/0.95
grid interaction	tie-line transmission capacity limits	$P_{grid,min}/P_{grid},max$	-500/800
demand response	maximum load adjustment capacity	$\Delta L_{min}, \Delta L_{max}$	-200/200

4.3 Results Analysis and Discussion

4.3.1 Comparative Analysis of Multi-Objective Optimization Results

The quantitative comparison of the scheduling results for the three schemes is presented in the table. Table 2. Comparison of results for different scheduling schemes.

Table 2. Comparison of scheduling results for different schemes.

Scheme	Economic Cost(10k Yuan)	Carbon Emission(ton)	Peak-Valley Diff(kW)
Scheme 1	1.44	6.88	1225.01
Scheme 2	1.76	6.65	997.12
Scheme 3	1.51	4.78	1077.67

In terms of economic performance, S1, serving as the single-objective economic benchmark, achieves the lowest cost (14,400 Yuan). After coordinating multiple objectives, S3 yields a cost of 15,100 Yuan, which is only 4.86% higher than that of S1, indicating that multi-objective optimization does not significantly compromise economic performance. S2 exhibits the poorest economic performance due to its rigid strategy, highlighting the value of intelligent optimization algorithms.

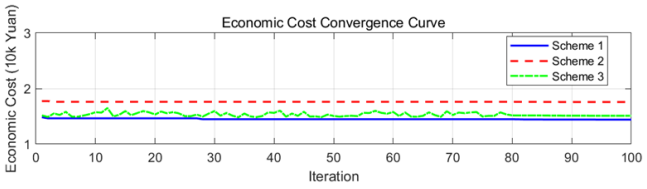

Fig. 5. Convergence curve of economic cost.

In terms of environmental performance, the carbon emissions of S3 (4.78 tons) are significantly lower than those of S1 and S2, achieving reductions of 30.52% and 28.12%, respectively. This indicates that the proposed strategy effectively promotes the integration of clean energy and reduces reliance on carbon-intensive energy sources by optimizing the output of the gas turbine and the charging/discharging schedule of the energy storage system.

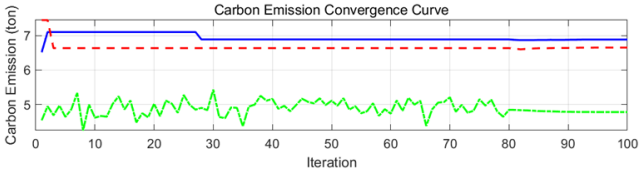

Fig. 6. Convergence curve of carbon emissions.

In terms of grid friendliness, the peak-valley load difference of S3 (1077.67 kW) is better than that of S1, which pursues economic performance alone, verifying its effectiveness in smoothing load fluctuations. Although it is slightly higher than that of S2, which adopts a fixed valley-filling strategy, this is a reasonable result of the Pareto trade-

off among the three objectives—economic performance, environmental performance, and stability—in S3.

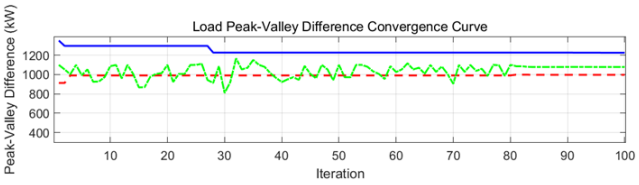

Fig. 7. Convergence curve of peak-valley load difference.

Scheme S3 simultaneously achieves a 30.52% reduction in carbon emissions and a 12.03% improvement in load curve smoothness at the cost of only a marginal 4.86% increase in economic cost, which fully demonstrates the significant advantages of the proposed multi-objective coordinated scheduling strategy in enhancing the comprehensive operational efficiency of virtual power plants.

4.3.2 Pareto Front and Scheduling Plan Analysis

Fig. 8 illustrates the three-dimensional distribution of the Pareto optimal solution set obtained by S3 in the objective space, along with its two-dimensional projections. It can be observed that the solution set is uniformly distributed, and there is a clear trade-off relationship among the three objectives (i.e., a reduction in economic cost is often accompanied by an increase in carbon emissions or load fluctuations). Decision-makers can flexibly select the final scheduling solution from this frontier based on actual policy or business preferences.

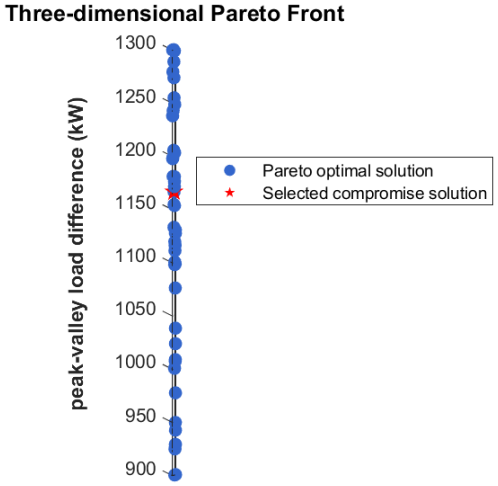

Fig. 8. Two-dimensional projections of the three-dimensional Pareto front.

In the detailed scheduling plan of Scheme S3 for a typical day, it can be observed that during the midday period when photovoltaic output is high, the energy storage system charges to absorb excess power while reducing electricity sales to the grid, thereby improving the self-consumption rate. During the evening peak load period when photovoltaic output drops to zero, the energy storage system and the gas turbine discharge in coordination, effectively supporting load demand and avoiding a sharp rise in the net load curve. Demand response mainly reduces load during peak-price periods, achieving synergy between peak shaving, valley filling, and economic incentives. This scheduling plan clearly reflects the intelligent coordinated interaction mechanism of source–storage–load–grid multiple resources driven by multi-objective optimization.

4.3.3 Algorithm Performance Comparison and Analysis

To validate the search performance of the DOA-NSGAII hybrid algorithm, it was compared with the classical multi-objective algorithms NSGA-II and MOEA/D under the same problem settings. Hypervolume (HV) and inverted generational distance (IGD) were adopted as evaluation metrics, and the statistical results after 30 independent runs are presented in Table 3.

Table 3. Performance comparison of different multi-objective algorithms (mean ± standard deviation)

Algorithm	Hypervolume (HV)	Inverted Generational Distance (IGD)	Runtime (s)
NSGA-II	0.712 ±0.021	0.085 ± 0.006	45.2
MOEA/D	0.698 ±0.025	0.091 ± 0.008	52.7
DOA-NSGAII	0.769 ±0.018	0.061 ± 0.005	58.3

The DOA-NSGAII algorithm proposed in this paper significantly outperforms the compared algorithms in terms of both HV and IGD metrics (a larger HV and a smaller IGD indicate higher solution set quality), demonstrating that the "dream exploration" and "memory consolidation" mechanisms of DOA effectively enhance the algorithm's global search capability and its ability to escape local optima, thereby enabling the discovery of Pareto solution sets with higher quality and better distribution. Although the runtime is slightly increased, the improvement in solution quality is substantial.

V. CONCLUSION

This study constructs a virtual power plant (VPP) model incorporating wind power, photovoltaics, gas turbines, energy storage systems, and price-based demand response, and proposes a hybrid intelligent solution strategy based on an improved Dream Optimization Algorithm (DOA) and the NSGA-II framework to address the multi-objective coordinated scheduling problem. Through

rigorous mathematical modeling, algorithm design, and simulation analysis, an efficient hybrid solution framework suitable for complex VPP optimization is developed. This study innovatively integrates the global search mechanism of the novel metaheuristic algorithm—the Dream Optimization Algorithm (DOA)—with the elitist selection strategy of the well-established multi-objective evolutionary algorithm NSGA-II, forming the DOA-NSGAII hybrid optimizer. This framework effectively addresses the challenges posed by the high-dimensional decision space, complex constraint coupling, and conflicting objectives in VPP scheduling. The resulting Pareto optimal solution set exhibits strong convergence and distribution performance, providing a reliable set of solutions for multi-criteria decision-making.

The validity and advantages of the Dream Optimization Algorithm in engineering optimization problems are verified. By simulating bio-inspired mechanisms such as "group-based memory," "selective forgetting," and "cross-individual information sharing," the algorithm demonstrates an excellent balance between global exploration and local exploitation when solving nonlinear, multi-peak scheduling models. Its integration with NSGA-II allows the search process to be guided by Pareto dominance, thereby systematically approaching the true Pareto front rather than becoming trapped in single-objective local optima.

The significant value of multi-objective coordinated scheduling in enhancing the comprehensive performance of VPPs is empirically demonstrated. Simulation results show that compared with the single-objective economic optimization scheme (Scheme S1), the proposed multi-objective optimization scheme (Scheme S3) achieves substantial gains-reducing carbon emissions by 30.5% and narrowing the peak-valley load difference by 12.0%—at the cost of only a marginal 4.9% increase in economic cost. This result quantitatively proves that intelligent coordinated optimization can effectively reconcile the inherent conflicts among economic efficiency, environmental performance, and system stability in VPP operation, achieving a Pareto improvement in overall operational effectiveness.

This study systematically elaborates the complete workflow for adapting the DOA algorithm to a specific engineering optimization problem, including decision variable encoding, hybrid constraint handling (equality constraint repair and penalty function method), and multi-objective integration. This provides a reproducible paradigm for the application of metaheuristic algorithms to similar complex system optimization problems.

ACKNOWLEDGEMENTS

This work was supported by the Research Funding of GDUPT, Research on Heat Transfer Enhancement of Heat Sink by Inverse Calculation Design Method (No. 2019rc074).

REFERENCES

[1] Qiu, Z., Zhang, X., Han, Z., Chen, F., Luo, Y., & Zhang, K. (2024). Power allocation optimization strategy for multiple virtual power plants with diversified distributed flexibility resources. *IET Renewable Power Generation*, 18(16), 4034–4046.

[2] Yao, L., Zhao, K., Shen, J., Xu, L., & Shen, L. (2026). Coordinated capacity configuration method for distributed resources of virtual power plants considering time-varying power coupling. *Energies*, 19(3), 614.

[3] Masiello, A., Borden, T., Buechler, N., Chassin, D., Giri, J., Hines, P., Kalsi, K., Lian, J., Liu, G., Mather, B., McJunkin, T., O'Brien, J., Palmintier, B., Pradhan, A., Rikos, E., & Vyakaranam, B. (2025). Deployment of virtual power plants for electrification enablement: Increasing hosting capacity to support electrification. *IEEE Electrification Magazine*, 13(1), 84–89.

[4] Othman, M. M., El-Khattam, W., & Hegazy, Y. G. (2023). Optimal siting and sizing of distributed generation in distribution networks considering hosting capacity. *International Journal of Electrical Power & Energy Systems*, 147, 108835.

[5] Pirouzi, A., & Aghaei, J. (2025). Risk-averse energy management of a water-heat-power virtual energy hub considering hosting capacity and Volt-VAR control of distribution network. *Energy*, 318, 134949.

[6] Ismael, S. M., Abdel Aleem, S. H. E., Abdelaziz, A. Y., & Zobaa, A. F. (2024). Review on hosting capacity of distributed energy resources: Analysis of the state of the art and future challenges. *Renewable and Sustainable Energy Reviews*, 189, 113908.

[7] Molina-Garcia, A., Mastromauro, R. A., Garcia-Sanchez, T., Pizzi, M., & Stasi, S. (2022). Distributed energy resources integration: A review of hosting capacity assessment methodologies. *IEEE Access*, 10, 124456–124481.

[8] Yang, Y., & Xu, Q. (2024). Optimal capacity allocation of energy storage in virtual power plants considering dynamic time-of-use pricing and conditional value-at-risk. *Journal of Energy Storage*, 82, 110518.

[9] Hosseini, E., Al-Ghaili, A. M., Kadir, D. H., Othman, M., & Yusof, R. (2024). Meta-heuristics and deep learning for energy applications: Review and open research challenges (2018–2023). *Energy Strategy Reviews*, 53, 101409.

[10] Lang, Y., & Gao, Y. (2025). Dream optimization algorithm (DOA): A novel metaheuristic optimization algorithm inspired by human dreams and its applications to real-world engineering problems. *Computer Methods in Applied Mechanics and Engineering*, 436, 117718.